ISSN 0021-3640, JETP Letters, 2019, Vol. 109, No. 6, pp. 358–363. © Pleiades Publishing, Inc., 2019.

FIELDS, PARTICLES, AND NUCLEI

Dimuon Resonance Near 28 GeV and the Muon Anomaly[1]

S. I. Godunov[a, b, *], V. A. Novikov[a, c, d, **], M. I. Vysotsky[a, c, d, *], and E. V. Zhemchugov[a, c, ****]**

[a] *Institute for Theoretical and Experimental Physics, Moscow, 117218 Russia*

[b] *Novosibirsk State University, Novosibirsk, 630090 Russia*

[c] *National Research Nuclear University MEPhI (Moscow Engineering Physics Institute), Moscow, 115409 Russia*

[d] *National Research University Higher School of Economics, Moscow, 101978 Russia*

**e-mail: sgodunov@itep.ru*

***e-mail: novikov@itep.ru*

****e-mail: vysotsky@itep.ru*

*****e-mail: zhemchugov@itep.ru*

Received February 4, 2019; revised February 4, 2019; accepted February 5, 2019

We demonstrate that the resonance recently observed by the CMS collaboration can be responsible for the deviation of the experimentally measured muon anomalous magnetic moment from its theoretical value.

DOI: 10.1134/S002136401906002X

1. INTRODUCTION

The CMS collaboration has recently reported a peak at invariant mass

$$m_X = (28.3 \pm 0.4)\ \text{GeV} \tag{1}$$

of $\mu^+\mu^-$ pairs produced in association with b jet in pp-collisions at the Large Hadron Collider (LHC) [1]. The peak appeared in the 8 TeV data with 19.7 fb^{-1} of integrated luminosity, while no significant excess was found in the 13 TeV data with 35.9 fb^{-1} of integrated luminosity.[2] The observation was made for two event categories with different cuts on jets directions with the local significances of 4.2 and 2.9 standard deviations (see [1] for the details). The fiducial cross section for both categories is at the level of 4 fb. Signal selection efficiency can strongly depend on the production process, so to evaluate the total $\sigma \times \mathrm{Br}(X \to \mu^+\mu^-)$ a particular model is required. The CMS paper does not study any specific model, so only the fiducial cross sections were provided.

The reported width of the peak is

$$\Gamma_X^{\text{exp}} = (1.8 \pm 0.8)\ \text{GeV}, \tag{2}$$

which is several times larger than the expected mass resolution for a dimuon system $\sigma_{\mu\mu} = 0.45$ GeV.

We shall study whether the resonance X (if its existence will be confirmed in the future) can explain the deviation of the measured value of the muon anomalous magnetic moment $a_\mu \equiv (g-2)_\mu/2$ from the Standard Model value

$$\delta a_\mu \equiv a_\mu^{\text{exp}} - a_\mu^{\text{SM}} = \begin{cases} (31.3 \pm 7.7) \times 10^{-10}, \text{ see [2]}, \\ (26.8 \pm 7.6) \times 10^{-10}, \text{ see [3]}. \end{cases} \tag{3}$$

In the following numerical estimates, we will use the average of these two values:

$$\delta a_\mu = (29 \pm 8) \times 10^{-10}. \tag{4}$$

2. X CONTRIBUTIONS TO $\delta \mathbf{a}_\mu$

Let us consider the Standard Model extended with a field X. Its contribution to the muon anomalous magnetic moment depends on X spin. We will consider the following four possibilities: scalar S, pseudoscalar P, vector V, axial vector A. Their coupling to muons is described by the following terms in the Lagrangian:

$$\begin{aligned} \Delta\mathcal{L}_{S\mu\mu} &= Y_{S\mu\mu}\bar{\mu}\mu S \quad \text{(scalar } X\text{)}, \\ \Delta\mathcal{L}_{P\mu\mu} &= iY_{P\mu\mu}\bar{\mu}\gamma_5\mu P \quad \text{(pseudoscalar } X\text{)}, \\ \Delta\mathcal{L}_{V\mu\mu} &= Y_{V\mu\mu}\bar{\mu}\gamma_\mu\mu V_\mu \quad \text{(vector } X\text{)}, \\ \Delta\mathcal{L}_{A\mu\mu} &= Y_{A\mu\mu}\bar{\mu}\gamma_\mu\gamma_5\mu A_\mu \quad \text{(axial vector } X\text{)}. \end{aligned} \tag{5}$$

[1] The article is published in the original.

[2] At 13 TeV, the excess can be hidden by the rapid growth of the background mainly provided by $t\bar{t}$ events (V.B. Gavrilov, private communication).

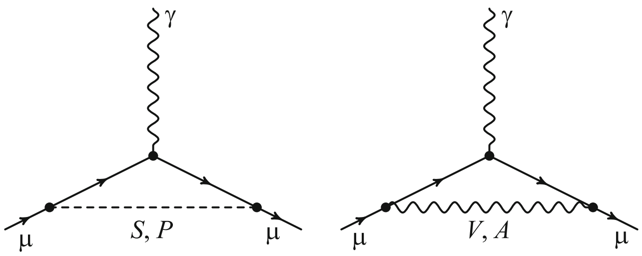

(a) scalar and pseudoscalar X

(b) vector and axial vector X

Fig. 1. One-loop contribution to δa_μ from (a) scalar and pseudoscalar X and (b) vector and axial vector X.

An exchange of X contributes at one loop to a_μ (see Fig. 1). The following results were obtained in [4, Eq. (260)]:

$$\delta a_\mu^S = \frac{Y_{S\mu\mu}^2}{4\pi^2}\left(\frac{m_\mu}{m_X}\right)^2\left[\ln\frac{m_X}{m_\mu} - \frac{7}{12}\right] \quad (\text{scalar } X), \tag{6}$$

$$\delta a_\mu^P = \frac{Y_{P\mu\mu}^2}{4\pi^2}\left(\frac{m_\mu}{m_X}\right)^2\left[-\ln\frac{m_X}{m_\mu} + \frac{11}{12}\right] \quad (\text{pseudoscalar } X), \tag{7}$$

$$\delta a_\mu^V = \frac{Y_{V\mu\mu}^2}{4\pi^2}\left(\frac{m_\mu}{m_X}\right)^2 \times \frac{1}{3} \quad (\text{vector } X), \tag{8}$$

$$\delta a_\mu^A = \frac{Y_{A\mu\mu}^2}{4\pi^2}\left(\frac{m_\mu}{m_X}\right)^2 \times \left(-\frac{5}{3}\right) \quad (\text{axial vector } X), \tag{9}$$

where $m_X \gg m_\mu$ is supposed. Only the scalar and vector X can resolve the discrepancy (4). Equating (4) to δa_μ^S and δa_μ^V results in

$$\begin{aligned} Y_{S\mu\mu} &= 0.041 \pm 0.006, \\ Y_{V\mu\mu} &= 0.16 \pm 0.02. \end{aligned} \tag{10}$$

In this case, the $X \to \mu^+\mu^-$ decay width

$$\begin{aligned} \Gamma(S \to \mu^+\mu^-) &= \frac{Y_{S\mu\mu}^2}{8\pi} m_X \left(1 - \frac{4m_\mu^2}{m_X^2}\right)^{3/2} \\ &= (1.8 \pm 0.5)\ \text{MeV}, \end{aligned} \tag{11}$$

$$\Gamma(V \to \mu^+\mu^-) = \frac{Y_{V\mu\mu}^2}{8\pi} m_X \sqrt{1 - \frac{4m_\mu^2}{m_X^2}} = (28 \pm 8) \quad \text{MeV},$$

and the corresponding branching ratios

$$\begin{aligned} \text{Br}(X \to \mu^+\mu^-) &= \frac{\Gamma(X \to \mu^+\mu^-)}{\Gamma_X^{(\text{exp.})}} \\ &= \begin{cases} (1.0 \pm 0.5) \times 10^{-3} & \text{for } S \to \mu^+\mu^-, \\ (1.5 \pm 0.8) \times 10^{-2} & \text{for } V \to \mu^+\mu^-. \end{cases} \end{aligned} \tag{12}$$

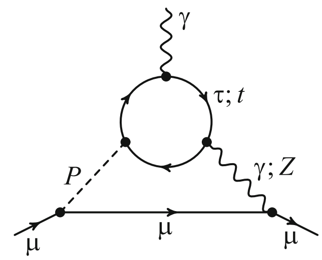

Fig. 2. Two-loop contribution of P to δa_μ.

Since the uncertainty in the measurement of Γ_X is rather large, the $X \to \mu^+\mu^-$ decay can dominate or even be the only decay of X.

Another possibility is that X can decay to other particles. For the scalar, such a small branching ratio can be naturally explained if S couples to $\tau^+\tau^-$ as well, and the coupling constants are proportional to μ and τ masses correspondingly. Then

$$\begin{aligned} \Gamma(S \to \tau^+\tau^-) &= \left(\frac{m_\tau}{m_\mu}\right)^2 \Gamma\left(S \to \mu^+\mu^-\right) \\ &= (0.52 \pm 0.15)\ \text{GeV}, \end{aligned} \tag{13}$$

which is in agreement with the reported value (2).

One of the most natural generalizations of the Standard Model is the model with additional heavy Higgs doublet, the so-called two Higgs doublets model (2HDM). Quite unexpectedly, the leading contributions to a_μ in this model for some values of parameters arise at the two-loop level (see Fig. 2), and light spin zero particle is needed to compensate the two-loop suppression [5–14]. It was found that a light pseudoscalar boson P with strong couplings to leptons could explain the current value of δa_μ (4). According to a recent paper [15], in a very small parameter region around $m_A = 20$ GeV the extra contribution to a_μ even exceeds the one needed to explain deviation (4). That is why it looks very appealing to identify the resonance found in [1] as the pseudoscalar boson P from 2HDM, resolving simultaneously the problem with muon anomaly. For this reason, we will not discard pseudoscalar P from consideration yet.

3. Z DECAYS AND X

If X is responsible for the muon anomaly then we know X coupling to muons, see Section 2. In this section, we are going to investigate how X modifies Z boson properties.

The width of Z decay to a fermion–antifermion pair and a pseudoscalar is [16]

$$\Gamma(Z \to f\bar{f}X) = \frac{\alpha}{128\pi^2}\frac{m_Z}{\sin^2\theta_W\cos^2\theta_W}\frac{N_c}{3} \times Y^2_{Xf\bar{f}}((g_A^2 + g_V^2)F_1 + (g_V^2 - g_A^2)F_2), \quad (14)$$

where N_c is the number of fermion colors, g_V and g_A are the axial and vector couplings of the fermion to the Z boson ($g_V = T_3$, $g_A = T_3 - 2Q\sin^2\theta_W$, T_3 is the third component of the weak isospin, and Q is the electric charge of the fermion),

$$F_1 = -2(1+3a)\ln a + \frac{1}{3}(1-a)(a^2 - 8a - 17),$$

$$F_2 = 2a(5+3a)\ln a - \frac{1}{3}(1-a)(a^2 - 44a - 5) + 4a^2\left[\frac{1}{2}\ln^2 a - \ln a\ln(1+a) + \mathrm{Li}_2\left(\frac{a}{1+a}\right) - \mathrm{Li}_2\left(\frac{1}{1+a}\right)\right], \quad (15)$$

$a = m_X^2/m_Z^2$, and $\mathrm{Li}_2(x)$ is the dilogarithm,

$$\mathrm{Li}_2(x) = -\int_0^x \frac{\ln(1-z)}{z}dz.$$

In this formula, the fermion is assumed to be massless, and in this limit, it also works for the scalar X.

The X particle will provide an extra contribution to $Z \to 4\mu$ decay through the following process: $Z \to \mu^+\mu^- X(\to \mu^+\mu^-)$. According to (14),

$$\Gamma(Z \to \mu^+\mu^- X) = 6.4 \times 10^{-5} \times Y^2_{S\mu\mu}\ \mathrm{GeV} \approx 105\ \mathrm{eV}, \quad (16)$$

where the value of $Y_{S\mu\mu}$ from (10) was substituted. Hence,

$$\mathrm{Br}(Z \to \mu^+\mu^- X(\to \mu^+\mu^-)) \approx 4.2 \times 10^{-8}\mathrm{Br}(X \to \mu^+\mu^-), \quad (17)$$

and even for $\mathrm{Br}(X \to \mu^+\mu^-) = 1$ it is one order of magnitude less than the experimental error: $\mathrm{Br}(Z \to 4\ell) = (3.5 \pm 0.4) \times 10^{-6}$ [17].

The width of X of the order of 1 GeV may be explained by $X \to \tau^+\tau^-$ and/or $X \to \nu\bar{\nu}$ decays. The upper limit on the $Y_{X\tau\tau}$ coupling can be obtained from the results of the DELPHI collaboration on the search of $Z \to \tau^+\tau^- h(\to \tau^+\tau^-)$ decays. According to [18, Fig. 11], the value of $Y_{X\tau\tau} = 100m_\tau/v \approx 0.7$ is allowed at 95% C.L., where $v \approx 246$ GeV is the Higgs boson expectation value. In this case, $\Gamma_X \approx 0.6$ GeV for both the scalar and pseudoscalar X, which is in agreement with the estimate (13).

The $X \to \nu\bar{\nu}$ decay increases the invisible Z boson width by the quantity

$$\Gamma(Z \to \nu\bar{\nu}X) = 0.4Y^2_{X\nu\nu}\ \mathrm{MeV}. \quad (18)$$

Since the experimental uncertainty in $\Gamma(Z \to \text{invisible})$ is about 1.5 MeV, the value of $Y_{X\nu\bar{\nu}}$ of the order of one is allowed leading to a GeV width of $X \to \nu\bar{\nu}$ decay.

Thus, we demonstrate that measured with high accuracy Z boson decay probabilities do not contradict the existence of relatively light X particle.

Let us note that X exchange leads to one loop corrections to the partial widths of $Z \to \ell\ell$ decays. In the recent paper [19] devoted to (pseudo)scalar explanations of the $g - 2$ anomaly, the bounds from these corrections were analyzed. The strongest bound comes from $Z \to \tau\tau$ decays, but the correction is within the experimental error for the value $Y_{X\tau\tau} = 0.7$ according to Eq. (10) from [19]. However, we doubt these results of paper [19] since its model is non-renormalizable. The axial coupling constant $Z\ell\ell$ (unlike vector one) gets infinite contribution at one loop level. For a reliable analysis of the radiative corrections to $Z \to \ell\ell$ width, a renormalizable extension of the Standard Model incorporating X is needed.

4. CAN X BE PRODUCED VIA RADIATION FROM b QUARK?

The X boson is seen by the CMS in association with at least one b-tagged jet. Let us consider the Standard Model extended with a boson X coupled to muons and b quarks. Let the coupling of X to b-quarks be described by interactions analogous to (5):

$$\begin{aligned}
\Delta\mathcal{L}_{Sbb} &= Y_{Sbb}\bar{b}bS \quad \text{(scalar } X\text{)},\\
\Delta\mathcal{L}_{Pbb} &= iY_{Pbb}\bar{b}\gamma_5 bP \quad \text{(pseudoscalar } X\text{)},\\
\Delta\mathcal{L}_{Vbb} &= Y_{Vbb}\bar{b}\gamma_\mu bV_\mu \quad \text{(vector } X\text{)},\\
\Delta\mathcal{L}_{Abb} &= Y_{Abb}\bar{b}\gamma_\mu\gamma_5 bA_\mu \quad \text{(axial vector } X\text{)}.
\end{aligned} \quad (19)$$

In this case, X is produced mainly by radiation from b quark.

In [1], the CMS collaboration reports fiducial cross sections for two event categories. In both cases exactly two jets with high p_T are required, one of which is b-tagged, and the b-tagged jet has to be in the barrel region. The main difference between the categories is in the direction of the untagged jet: it can be in either the endcap or the barrel regions. Below, the first event category will be considered since it possesses the highest significance of 4.2 standard deviations. The corresponding fiducial cross section is

$$\sigma_{\mathrm{fid.1}} = (4.1 \pm 1.4)\ \mathrm{fb}, \quad (20)$$

and the cuts are summarized in Table 1 from [1].

To calculate the cross section of X production at the LHC, CalcHEP 3.6.30 [20] was used. CalcHEP

Table 1. Fiducial cross sections $\sigma^{\rm fid}$ for the $pp \to bX + jet + ...$ reaction and its subprocesses for $Y_{Xb\bar{b}} = 0.01$ and $Y_{X\mu\mu} = 1$ at $\sqrt{s} = 8$ TeV. We took such a small value of Y_{Xbb} to suppress multiple X exchanges. The errors correspond to integration errors reported by CalcHEP. When summing up one should multiply the value by two if there are two reactions in left column. The second column corresponds to the multiplicity due to the two possibilities of the quark and its parent proton combination and due to the fact that each b jet can be directed into barrel if there are more than one b jet

Subprocess	Multiplicity	$\sigma^{\rm fid} \times 10^5$ [pb]			
		S	P	V	A
$bu \to ub\mu\mu$ $\bar{b}u \to u\bar{b}\mu\mu$	2	5.23(2)	5.22(2)	16.0(1)	16.3(1)
$b\bar{u} \to \bar{u}b\mu\mu$ $\bar{b}\bar{u} \to \bar{u}\bar{b}\mu\mu$	2	0.298(1)	0.293(2)	0.86(1)	0.89(1)
$bd \to db\mu\mu$ $\bar{b}d \to d\bar{b}\mu\mu$	2	2.30(1)	2.30(1)	6.91(4)	7.14(4)
$b\bar{d} \to \bar{d}b\mu\mu$ $\bar{b}\bar{d} \to \bar{d}\bar{b}\mu\mu$	2	0.359(2)	0.355(2)	1.05(1)	1.08(1)
$bs \to sb\mu\mu$ $\bar{b}s \to s\bar{b}\mu\mu$	2	0.209(2)	0.202(1)	0.593(4)	0.617(5)
$b\bar{s} \to \bar{s}b\mu\mu$ $\bar{b}\bar{s} \to \bar{s}\bar{b}\mu\mu$	2	0.206(2)	0.205(1)	0.602(5)	0.618(6)
$bc \to cb\mu\mu$ $\bar{b}c \to c\bar{b}\mu\mu$	2	0.113(1)	0.114(1)	0.336(2)	0.350(3)
$b\bar{c} \to \bar{c}b\mu\mu$ $\bar{b}\bar{c} \to \bar{c}\bar{b}\mu\mu$	2	0.115(1)	0.114(1)	0.337(3)	0.340(2)
$bg \to gb\mu\mu$ $\bar{b}g \to g\bar{b}\mu\mu$	2	7.42(8)	7.54(8)	22.1(2)	23.4(3)
$bb \to bb\mu\mu$ $\bar{b}\bar{b} \to \bar{b}\bar{b}\mu\mu$	1	0.146(3)	0.142(2)	0.36(1)	0.45(1)
$gg \to b\bar{b}\mu\mu$	2	5.19(8)	5.11(7)	21.3(3)	20.6(5)
$b\bar{b} \to b\bar{b}\mu\mu$	4	0.082(1)	0.085(3)	0.286(3)	0.222(3)
$u\bar{u} \to b\bar{b}\mu\mu$	4	0.0636(3)	0.0631(3)	0.182(2)	0.184(2)
$d\bar{d} \to b\bar{b}\mu\mu$	4	0.0323(4)	0.0309(3)	0.0886(9)	0.0881(9)
$s\bar{s} \to b\bar{b}\mu\mu$	4	0.0036(2)	0.0039(1)	0.0103(1)	0.0106(1)
$c\bar{c} \to b\bar{b}\mu\mu$	4	0.00160(5)	0.00165(1)	0.0044(1)	0.0041(2)
All		76.4(4)	76.6(4)	241(1)	247(1)

parameters were updated to their modern values according to [17]. MMHT2014nnlo68cl [21] from the Les Houches PDF library [22] was used as the set of parton distribution functions.

Calculated cross sections for the first event category cuts (fiducial cross sections) are presented in Table 1. Thus, the events with two b jets correspond to approximately one sixth of the reported fiducial cross section (20).

The search for the light pseudoscalar boson, which is produced in association with two b jets and decays into two muons, was performed at $\sqrt{s} = 8$ TeV in the previous CMS paper [23]. It was found that $\sigma(pp \to b\bar{b}P){\rm Br}(P \to \mu\mu) > 350$ fb is excluded at 95% C.L. for $M_P = 30$ GeV. To compare the observed excess with this result, we are going to separate the processes with two b jets in the final state and find the

Table 2. Cross sections for the $pp \to bbX + \ldots$ reaction and its subprocesses for $Y_{Xb\bar{b}} = 0.01$ and $Y_{X\mu\mu} = 1$ at $\sqrt{s} = 8$ TeV. The errors correspond to integration errors reported by CalcHEP

Subprocess	Multiplicity	σ [pb], S	σ [pb], P	σ [pb], V	σ [pb], A
$bb \to bb\mu\mu$ $\bar{b}\bar{b} \to \bar{b}\bar{b}\mu\mu$	1	0.024(2)	0.025(1)	0.048(3)	0.061(2)
$gg \to b\bar{b}\mu\mu$	1	1.66(3)	1.96(3)	5.68(9)	5.57(3)
$b\bar{b} \to b\bar{b}\mu\mu$	2	0.034(3)	0.029(1)	0.072(1)	0.056(2)
$u\bar{u} \to b\bar{b}\mu\mu$	2	0.00109(1)	0.00091(1)	0.00250(1)	0.00279(1)
$d\bar{d} \to b\bar{b}\mu\mu$	2	0.00077(1)	0.000640(1)	0.001735(3)	0.001957(6)
$s\bar{s} \to b\bar{b}\mu\mu$	2	0.000267(1)	0.000217(2)	0.000554(1)	0.000639(1)
$c\bar{c} \to b\bar{b}\mu\mu$	2	0.000133(1)	0.000107(1)	0.000270(1)	0.000315(1)
All with 2b jets		1.78(3)	2.07(2)	5.93(9)	5.82(3)

total cross section that corresponds to the observed fiducial one. In order to do that we have to find the cut efficiency for the subprocesses with two b jets in the final state; i.e., we need the total cross sections for these subprocesses. The CalcHEP results for these cross sections are summarized in Table 2.

With the help of the data from Table 1 we can find the contribution of each subprocess into the reported fiducial cross section (20) without knowing the coupling constants Y_{Xbb} and $Y_{X\mu\mu}$:

$$\sigma^{\text{fid}}(\text{subprocess}) = \frac{\sigma^{\text{fid}}(\text{subprocess})\big|_{Y_{Xbb}=10^{-2},Y_{X\mu\mu}=1}}{\sigma^{\text{fid}}(\text{All})\big|_{Y_{Xbb}=10^{-2},Y_{X\mu\mu}=1}} \times \sigma_{\text{fid.1}}. \tag{21}$$

Signal selection efficiency ε depends on the subprocess. We will calculate it using data from Tables 1 and 2:

$$\varepsilon(\text{subprocess}) = \frac{\sigma^{\text{fid}}(\text{subprocess})\big|_{Y_{Xbb}=10^{-2},Y_{X\mu\mu}=1}}{\sigma(\text{subprocess})\big|_{Y_{Xbb}=10^{-2},Y_{X\mu\mu}=1}}. \tag{22}$$

Then we obtain the cross section for individual subprocesses:

$$\sigma(\text{subprocess}) = \frac{\sigma^{\text{fid}}(\text{subprocess})}{\varepsilon(\text{subprocess})} = \frac{\sigma(\text{subprocess})\big|_{Y_{Xbb}=10^{-2},Y_{X\mu\mu}=1}}{\sigma^{\text{fid}}(\text{All})\big|_{Y_{Xbb}=10^{-2},Y_{X\mu\mu}=1}} \times \sigma_{\text{fid.1}}. \tag{23}$$

For the cross section of subprocesses with two b jets in final state we get

$$\sigma(pp \to X + 2b\text{-jets}) \times \text{Br}(X \to \mu\mu) = \sum_{\text{subprocesses with } 2b \text{ jets}} \sigma(\text{subprocess}) = \frac{\sigma(\text{All with } 2b \text{ jets})\big|_{Y_{Xbb}=10^{-2},Y_{X\mu\mu}=1}}{\sigma^{\text{fid}}(\text{All})\big|_{Y_{Xbb}=10^{-2},Y_{X\mu\mu}=1}} \times \sigma_{\text{fid.1}} = \frac{2.07 \text{ pb}}{76.6 \times 10^{-5} \text{ pb}} \times 4.1 \text{ fb} \approx 11 \text{ pb}, \tag{24}$$

where in the last line we substituted the values for the pseudoscalar. In the cases of S, V, and A the results are approximately the same. Let us note that according to A.N. Nikitenko (private communication) the cut efficiency for the whole first event category in the case of pseudoscalar is approximately 2.7×10^{-4}, so the total cross section is about 15 pb.

Substituting the data from Tables 1 and 2 into Eq. (24), we get $\sigma(pp \to X + 2b\text{-jets}) \times \text{Br}(X \to \mu\mu)$ much larger than the bound at the level of 350 fb observed in the previous CMS paper [23] for pseudoscalar. As far as different angular distributions cannot explain this huge difference in total cross sections, we conclude that the mechanism discussed in this section cannot be responsible for X production at the LHC for any of S, P, V, A cases.

In the 2HDM discussed in Section 2 pseudoscalar P is produced mainly by radiation from b quark, just like it is described in this section. Therefore, the 2HDM cannot explain experimental data.

5. CONCLUSIONS

An extra scalar or vector can describe the resonance discovered in [1], and simultaneously resolve the disagreement between the Standard Model result for the muon anomalous magnetic moment and its measured value. The total width of the resonance observed in the experiment can be explained by

$X \to \tau\tau$ and $X \to \nu\nu$ decays. These are the main results of this work.

Though X was found in association with at least one b jet, the simplest model of its production via radiating from b quark line contradicts the previous CMS paper [23]: while the cuts in the new paper are much stronger (mostly cuts on muons) the fiducial cross section is at the level of the upper limit on fiducial cross section from previous paper. To resolve this contradiction, stronger cuts on muons transverse momentum should not significantly diminish the number of events; i.e., X should be produced with high transverse momentum. This can be achieved if X is produced in decays of a heavy particle, for example, vector-like B quark via $\bar{B}_L b_R X$ interaction term. The construction of such a model is the subject of the future work.

Since the New Physics responsible for the observed resonance is connected to b quarks as well, it can explain the deviations from the Standard Model predictions observed in semileptonic B decays.

If the existence of X will be confirmed by future experimental data, it will be a strong additional argument in favor of muon collider construction.

We are grateful to V.B. Gavrilov, who has brought the CMS discovery to our attention, and to A.N. Nikitenko for valuable comments. We gratefully acknowledge discussions with R.B. Nevzorov. This work was supported by the Russian Foundation for Basic Research, project no. 16-02-00342. S.I. Godunov acknowledges the support of the Russian Foundation for Basic Research, project no. 16-32-60115.

REFERENCES

1. A. M. Sirunyan, A. Tumasyan, W. Adam, et al. (CMS), J. High Energy Phys. **11**, 161 (2018); arXiv:1808.01890 [hep-ex].
2. F. Jegerlehner, EPJ Web Conf. **166**, 00022 (2018); arXiv:1705.00263 [hep-ph].
3. M. Davier, A. Hoecker, B. Malaescu, and Z. Zhang, Eur. Phys. J. C **77**, 827 (2017); arXiv:1706. 09436 [hep-ph].
4. F. Jegerlehner and A. Nyffeler, Phys. Rep. **477**, 1 (2009); arXiv:0902.3360 [hep-ph].
5. D. Chang, W.-F. Chang, C.-H. Chou, and W.-Y. Keung, Phys. Rev. D **63**, 091301 (2001); arXiv:hep-ph/0009292[hep-ph].
6. A. Broggio, E. J. Chun, M. Passera, K. M. Patel, and S. K. Vempati, J. High Energy Phys. **11**, 058 (2014); arXiv:1409.3199[hep-ph].
7. E. J. Chun and J. Kim, J. High Energy Phys. **07**, 110 (2016); arXiv:1605.06298 [hep-ph].
8. L. Wang and X.-F. Han, J. High Energy Phys. **05**, 039 (2015); arXiv:1412.4874 [hep-ph].
9. T. Abe, R. Sato, and K. Yagyu, J. High Energy Phys. **07**, 064 (2015); arXiv:1504.07059 [hep-ph].
10. A. Crivellin, J. Heeck, and P. Stoffer, Phys. Rev. Lett. **116**, 081801 (2016); arXiv: 1507.07567 [hep-ph].
11. E. J. Chun, Z. Kang, M. Takeuchi, and Y.-L. S. Tsai, J. High Energy Phys. **11**, 099 (2015); arXiv:1507.08067 [hep-ph].
12. T. Han, S. K. Kang, and J. Sayre, J. High Energy Phys. **02**, 097 (2016); arXiv:1511.05162 [hep-ph].
13. V. Ilisie, J. High Energy Phys. **04**, 077 (2015); arXiv:1502.04199 [hep-ph].
14. A. Cherchiglia, P. Kneschke, D. Stöckinger, and H. Stöckinger-Kim, J. High Energy Phys. **01**, 007 (2017); arXiv:1607.06292 [hep-ph].
15. A. Cherchiglia, D. Stöckinger, and H. Stöckinger-Kim, Phys. Rev. D **98**, 035001 (2018); arXiv:1711.11567 [hep-ph].
16. A. Djouadi, P. M. Zerwas, and J. Zunft, Phys. Lett. B **259**, 175 (1991).
17. C. Patrignani, K. Agashe, G. Aielli, et al. (Particle Data Group), Chin. Phys. C **40**, 100001 (2016); 2017 update.
18. J. Abdallah, P. Abreu, W. Adam, et al. (DELPHI), Eur. Phys. J. C **38**, 1 (2004); arXiv:hep-ex/0410017 [hep-ex].
19. F. Abu-Ajamieh, arXiv:1810.08891 [hep-ph] (2018).
20. A. Belyaev, N. D. Christensen, and A. Pukhov, Comput. Phys. Commun. **184**, 1729 (2013); arXiv:1207.6082[hep-ph].
21. A. D. Martin, W. J. Stirling, R. S. Thorne, and G. Watt, Eur. Phys. J. C **63**, 189 (2009); arXiv:0901.0002 [hep-ph].
22. A. Buckley, J. Ferrando, S. Lloyd, K. Nordström, B. Page, M. Rüfenacht, M. Schönherr, and G. Watt, Eur. Phys. J. C **75**, 132 (2015); arXiv:1412.7420 [hep-ph].
23. A. M. Sirunyan, A. Tumasyan, W. Adam, et al. (CMS), J. High Energy Phys. **11**, 010 (2017); arXiv:1707.07283 [hep-ex].